CrossMark

NEURO

Self-controlled super-selective arterial spin labelling

Thomas Lindner[1] · Friederike Austein[1] · Olav Jansen[1] · Michael Helle[2]

Abstract

Objectives Arterial spin labelling (ASL) is a method of non-contrast-enhanced perfusion imaging that is generally based on the acquisition of two images which must be subtracted in order to obtain perfusion-weighted images. This is also the case for some flow territory mapping approaches that require the acquisition of two images for each artery of interest, thereby prolonging scan time and yielding largely redundant information. The aim of this study is to accelerate flow territory mapping using ASL by eliminating the acquisition of a control condition.

Methods Using super-selective ASL, only one artery of interest is tagged, while the contralateral arteries are in a state similar to the control condition. By using an arithmetic combination of the label images of all territories, selective images of flow territories can be obtained without the need to acquire an additional control condition. This approach for obtaining artery-selective perfusion-weighted images without acquiring a control condition is presented in this study and is referred to as "self-controlled super-selective ASL".

Results Quantitative perfusion measurements were similar to conventional super-selective and non-selective perfusion imaging across all subjects.

Conclusion Super-selective arterial spin labelling can be performed without acquiring a control image.

Key Points
- *An accelerated method of flow territory mapping is presented.*
- *Super-selective arterial spin labelling is performed without a control condition.*
- *A new approach for calculating individual flow territories is presented.*
- *The presented technique is compared to established approaches.*
- *The outcome is similar to that using conventional techniques.*

Keywords Super-selective · Arterial spin labelling · Flow territory mapping · Self-control · Perfusion

✉ Thomas Lindner
Thomas.Lindner@uksh.de

Friederike Austein
Friederike.Austein@uksh.de

Olav Jansen
Olav.Jansen@uksh.de

Michael Helle
Michael.Helle@philips.com

1 Department of Radiology and Neuroradiology, University Hospital Schleswig-Holstein Campus Kiel, Arnold-Heller-Str. 3, 24103 Kiel, Germany

2 Philips GmbH Innovative Technologies Research Laboratories, Röntgenstraße 24-26, 22335 Hamburg, Germany

Introduction

Magnetic resonance (MR) perfusion imaging methods are widely used for the detailed investigation of intracranial arterial status and function [1, 2]. Arterial spin labelling (ASL) is an attractive approach, as no external contrast agent application is required. Furthermore, because MR does not involve any kind of ionising radiation, it is also suitable for follow-up measurements [3, 4]. Often, however, only the whole-brain perfusion can be depicted, which impedes the ability to draw conclusions about individual flow territories, but may be required in certain diseases [5]. With the use of MRI, the

application of specialised magnetisation preparation pulses allows for visualising blood flow originating from a single artery [6–8]. Selective ASL is most often used for selectively visualising the major brain-feeding arteries (internal carotid artery [ICA] or basilar artery [BA]), although imaging of smaller arteries is also possible [7].

Pseudo-continuous ASL (pCASL) is currently the recommended technique for use in perfusion studies [9, 10]. Additionally, modifications allow for selective labelling of individual arteries [6, 7]. ASL relies on the acquisition of two images, a label (inversion) and a control (no inversion) image. These images are subtracted to visualise only the difference signal of the labelled blood, while static tissue components are cancelled out. When using super-selective pCASL, the optimal situation during labelling would be that the arteries of interest are in the inversion state, while the non-labelled arteries and static tissue remain unchanged [7]. The label and control experiment are typically acquired using similar RF and gradient amplitudes to cancel out potential magnetisation transfer effects. The combination of a label and control acquisition for each individual artery, however, prolongs scan time. Therefore, the ability to eliminate the control condition in order to reduce overall scan time is an attractive feature. Various studies have proposed such approaches, which have included acquiring a single control condition, Hadamard encoding, Bayesian inference modelling and dual-inversion recovery [11–15].

In contrast to other approaches, with super-selective ASL, it can be assumed that only the artery of interest is in the label condition. The non-tagged arteries are in a control-like condition (pseudo-randomised states of spin magnetisation), depending on the distance to the labelling focus [7].

The aim of this work is thus to make use of this state present in selectively labelled images to present an accelerated method for artery-selective ASL. This process is referred to as "self-controlled super-selective ASL" or "self-controlled ss-ASL", as only the label images are used. The obtained images are then compared in terms of cerebral blood flow (CBF) to conventional super-selective and non-selective ASL.

Methods

Image calculation

In non-selective and super-selective ASL, images are obtained by subtracting the label from the control image. Through subtraction, the static tissue components are removed, while in blood, a difference signal remains. Using super-selective ASL, this calculation must be repeated for each artery.

In self-controlled ASL, no control condition is acquired, and the artery-selective images can be obtained using a combination of the two contralateral acquisitions,

with subtraction of the duplicate acquisition of the artery of interest, as follows:

$$RICA_{final} = (LICA + BA) - (RICA + RICA) \qquad (1)$$

$$LICA_{final} = (RICA + BA) - (LICA + LICA) \qquad (2)$$

$$BA_{final} = (RICA + LICA) - (BA + BA) \qquad (3)$$

RICA and LICA indicate the label images of the right and left carotid artery, respectively, and BA indicates the basilar artery. A schematic of the RICA calculation is presented in Fig. 1. In the flow territories of contralateral arteries, the calculation leads to a negative signal. These voxels are set to zero.

MR Experiments

The data acquired for this study were part of a general protocol for MRI pulse-sequence development approved by the local ethical committee. Volunteers gave written informed consent. The study population included six healthy volunteers (4 women and 2 men, mean age 24.8 years) with no known history of intracerebral pathologies. All experiments were performed on a Philips 3T Achieva MR scanner (Philips Healthcare, Best, The Netherlands) using a standard 32-channel head coil. For planning of selective ASL, the information regarding the position of the arteries was obtained via time-of-flight angiography [12].

The tagging and readout parameters were kept identical between the selective and non-selective approaches. The labelling duration was 1650 ms, and the post-labelling delay was 1600 ms. For selective labelling of the ICA and the BA, the additional gradient moments were 1.08 mT/m in G_x and G_y directions [16]. With the self-controlled approach, the labelling spot changes its position after each acquisition. These positions of the arteries of interest were chosen manually. The spot then "cycles" from the right ICA to the left ICA, then to the BA. This is repeated until all scan acquisitions (label images in self-controlled ss-ASL) are completed. Images of all three flow territories can thus be retrieved from a single scan [12]. Image acquisition was performed as single-shot multi-slice echo planar imaging (EPI) with 2.75×2.75 mm^2 in-plane resolution and 16 slices with 5-mm thickness covering 95 mm. The following parameters were used: field of view, 240×240 mm; TR/TE, 3847/13 ms; flip angle, 90°. In non-selective ASL, 40 acquisitions were performed (20 label/control pairs); for super-selective ASL, a total of 120 acquisitions were performed (20 label/control pairs for each artery); and for self-controlled ASL, 60 acquisitions (20 label images

Fig. 1. Calculations of the final images for the example of the right internal carotid artery. (a) Self-controlled super-selective ASL. (b) Conventional super-selective ASL. In both examples, the right internal carotid artery is visualised. The subscript "L" indicates label images and "C" control images, while "final" indicates the final calculated images. Note that black numbers represent blood signal and red numbers static tissue signal. In (a), all negative signal in the flow territories of the contralateral arteries (in this example LICA and BA) of the final image is artificially set to zero after the calculations (not shown)
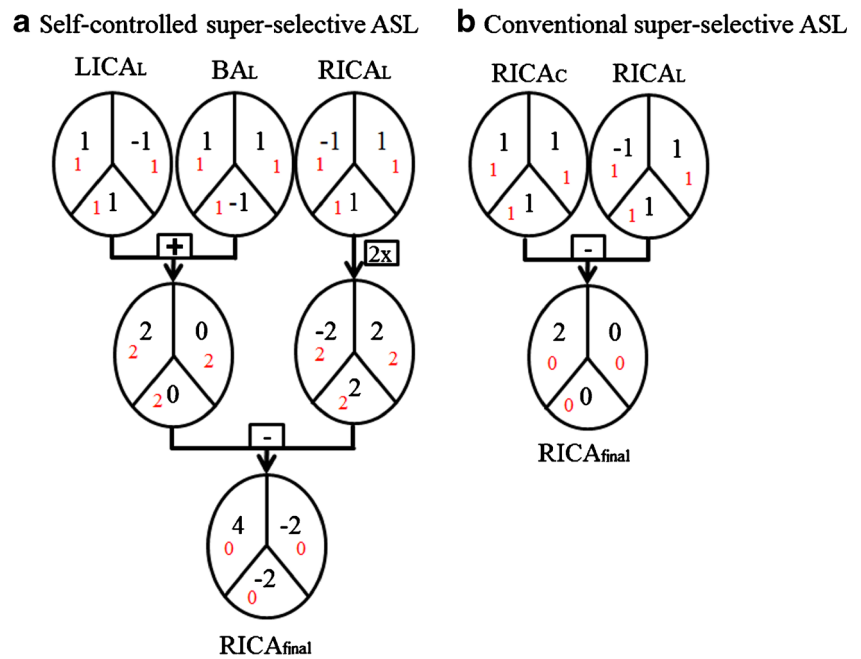
for each artery). Scan time was 14:36 min using super-selective ASL, 7:18 min with self-controlled ASL, and 4:52 min for non-selective ASL.

Image post-processing and data analysis

All images were exported and post-processed using Matlab R2013b (MathWorks, Natick, MA, USA). From the label images (and if existing, the control images), subtraction images were created either by a simple subtraction or by using formulas 1-3 for the respective flow territories.

For a quantitative measure of perfusion, the images were post-processed using the model recommended by the International Society for Magnetic Resonance in Medicine (ISMRM) Perfusion Study Group [9]:

$$CBF\ [ml/\min/100g] = \frac{6000^* \lambda^* \left(SI_{final}\right)^* e^{\frac{PLD}{T1_{blood}}}}{2^* \alpha^* T1_{blood}{}^* M_0{}^* \left(1 - e^{-\frac{\tau}{T1_{blood}}}\right)} \quad (4)$$

where SI_{final} is the signal intensity of the final processed (i.e. subtracted) images, λ is the blood–brain partition coefficient, α is the labelling efficiency, PLD is the post-labelling delay, $T1_{blood}$ is the T1 relaxation constant of blood, M_0 is the signal intensity of the M_0 image, and τ is the labelling duration.

By combining the images according to Fig. 1 (i.e. twice the label image of interest and two contralateral images) for calculating the vascular territories, rather than only two as in conventional (selective) ASL, the signal level of the contralateral images increases by the square root of 2, which needs to be accounted for [17]. For comparison of CBF in individual flow territories of the non-selective ASL images, conventional

super-selective ASL was used as mask to obtain the flow territory of the artery of interest.

To compare CBF values, the Pearson correlation coefficient (r) was calculated and ANOVA testing was performed based on the average values obtained from the individual flow territories.

Results

Image acquisition

Image acquisition was performed successfully in all volunteers, and no data sets had to be discarded due to movement or misplaced labelling foci. Figure 2 shows representative images of both quantitative CBF images of all flow territories (a) and relative CBF images of the RICA and a difference image of both (b). The difference image was created by subtracting the conventional image from the self-controlled ss-ASL. This image shows the difference in signal in the peripheral grey matter zones that is mostly image noise, indicating no major differences between the two methods (red arrows).

Data evaluation

Quantitative CBF measures were similar for conventional ASL, super-selective ASL and self-controlled ASL imaging. The results for each individual volunteer are listed in Table 1. The CBF values for all three methods differed by less than ± 5 ml/min/100 g for each artery. No major deviations were found
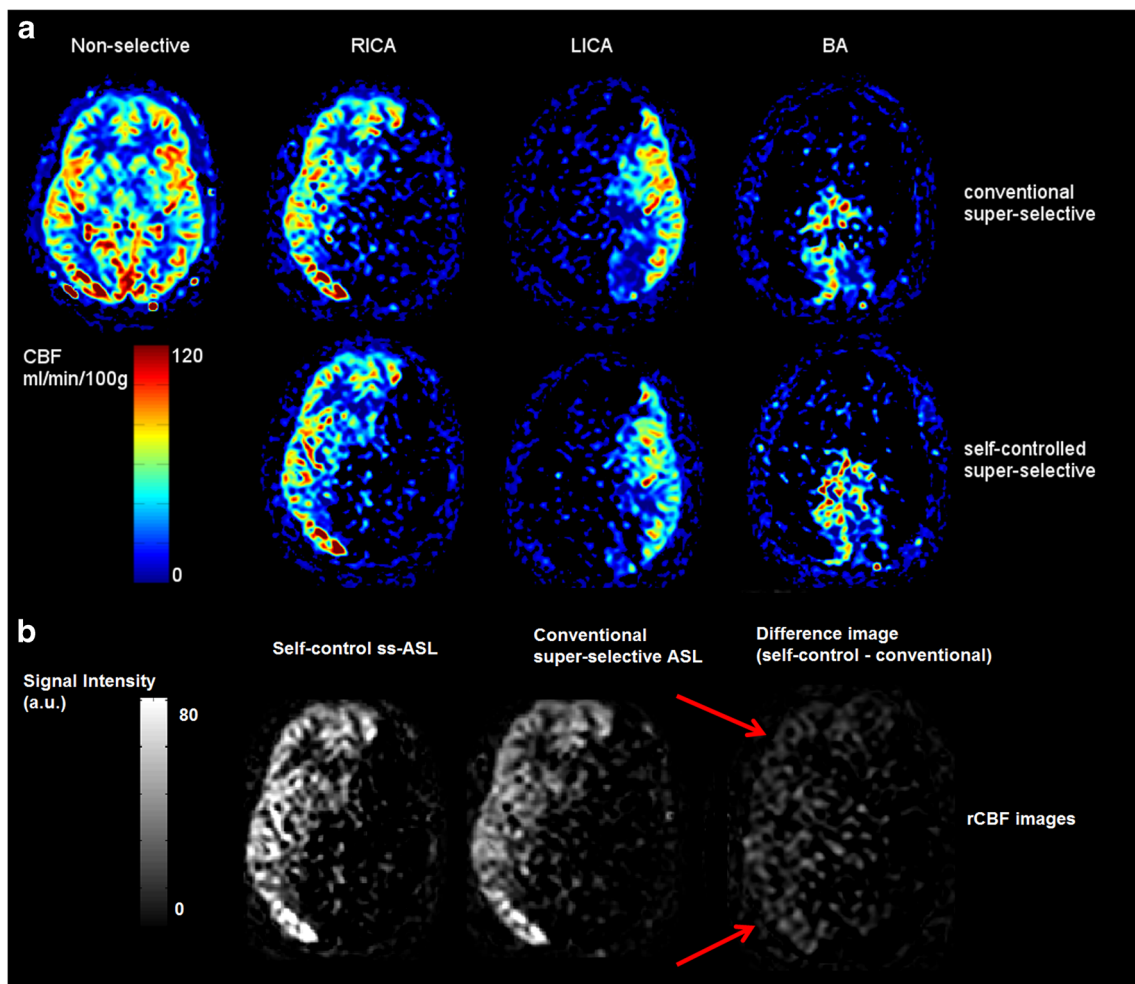
Fig. 2. (a) Representative images of one volunteer after quantification of CBF data. In the upper row, non-selective and conventional super-selective ASL images are presented. The bottom row shows self-controlled super-selective ASL images. Both the selectivity and the quantitative values appear similar in all approaches (b) Relative CBF (rCBF) images of the RICA showing the gain in SNR of self-controlled ss-ASL compared to the conventional approach, and a difference image of both approaches. The difference image shows differences in signal, which can be largely attributed to noise, indicating no significant differences between methods (red arrows)

in either of the carotid arteries, and the Pearson correlation coefficients appeared similar ($r = 0.97 – 0.98$).

Regarding the posterior circulation, both selective approaches displayed lower correlation compared to non-selective ASL ($r = 0.87$ for both), while the comparison between selective approaches showed a high correlation ($r = 0.99$).

Figure 3 shows the linear regression curves of the results alongside the Pearson correlation coefficient (r).

ANOVA testing showed an F-value of 0.076 for the RICA, 0.002 for the LICA and 0.131 for the BA, with the critical F-value at 3.682 for all tests.

Discussion

In this study, an approach for the accelerated visualisation of individual flow territories was proposed and evaluated in comparison to non-selective and conventional super-selective ASL.

This was achieved using an image decoding scheme in which the control acquisition was discarded. Generally, to obtain perfusion-weighted images using ASL, a label image is performed with a matching control image. The two images have the same signal except for the magnetic state of the inflowing labelled blood in order to subtract the static background tissue. In principle, in super-selective ASL, the gradients performed perpendicular to the labelling plane could cause adverse effects, so it is important to acquire a control image in which the same gradient pattern is used. Factors influencing the labelling efficiency and potential artefacts include the gradient scheme and the position of the labelling focus, as well as the strength of the additional gradients, which define the size of the labelling focus [7]. However, the need to acquire two matching images increases scan time, and the information in the control images is largely redundant.

Table 1 Quantitative CBF values (in ml/min/100 g brain tissue) obtained from all volunteers

	Non-selective		Super-selective		Self-controlled	
RICA						
	CBF	SD	CBF	SD	CBF	SD
Volunteer 1	48.17	11.99	49.49	13.26	48.76	12.66
Volunteer 2	47.84	8.32	45.56	10.43	46.72	8.96
Volunteer 3	52.45	9.47	53.76	13.71	53.41	9.79
Volunteer 4	44.81	13.76	46.75	10.80	48.61	13.32
Volunteer 5	59.13	10.99	58.25	9.98	62.12	12.85
Volunteer 6	39.09	13.43	36.86	14.05	39.90	8.27
Mean	48.58	11.33	48.45	12.04	49.92	10.98
SD	6.80	2.16	7.36	1.83	7.41	2.22
LICA						
Volunteer 1	50.16	8.15	51.21	11.69	51.12	11.03
Volunteer 2	40.14	9.57	42.43	11.23	40.63	15.00
Volunteer 3	54.44	12.63	55.97	11.92	53.76	9.44
Volunteer 4	46.52	11.99	46.19	12.27	49.04	9.92
Volunteer 5	62.13	11.61	61.12	11.54	63.13	12.55
Volunteer 6	42.16	8.17	40.25	11.58	39.06	10.86
Mean	49.26	10.35	49.53	11.71	49.46	11.47
SD	8.18	1.98	8.08	0.36	8.88	2.04
BA						
Volunteer 1	42.13	11.74	42.34	8.44	42.93	9.32
Volunteer 2	38.12	11.01	39.41	14.16	41.16	12.80
Volunteer 3	47.22	13.89	48.13	12.97	47.16	10.40
Volunteer 4	42.13	13.63	40.21	14.44	42.38	8.87
Volunteer 5	48.13	8.25	45.26	13.51	45.63	11.75
Volunteer 6	41.63	14.81	38.72	9.72	40.02	8.92
Mean	43.23	12.22	42.35	12.21	43.21	10.34
SD	3.77	2.41	3.70	2.51	2.71	1.63

The values of all three methods differ by less than ± 5 ml/min/100 g, which might be caused by minor malpositioning of the volunteers between the individual scans and physiological variations during the scans. *CBF* cerebral blood flow, *RICA* right internal carotid artery, *LICA* left internal carotid artery, *BA* basilar artery, *SD* standard deviation

Inaccurate subtraction of images could occur if the label and control condition do not correspond. This was not observed in an earlier study using a single control condition, and was also not observed in this work [12]. This was proven statistically by calculating the Pearson correlation coefficient, showing excellent correlation between methods. This finding indicates that the extra gradients applied do not need to be applied on the same position to produce adequate subtraction images [12]. Other sequence-related parameters should still remain the same for all acquisitions. The minor deviations of only ± 5 ml/min/100 g might be caused by malpositioning of the volunteers between the individual scans or movements during the scans. Furthermore, physiological variations due to overall long scan times are inevitable.

In the posterior circulation, the highest deviation occurred when the selective approaches were compared to non-selective ASL. These are most likely caused by reduced labelling efficiency due to geometric properties (smaller diameter) and different flow (slow flow), as both selective approaches show the same low *r* value compared to non-selective ASL, but with $r = 0.99$ in direct comparison. This might be circumvented by measuring the labelling efficiency for each individual artery [18].

Compared to non-selective acquisition, selective ASL measurements increase the scan time with the number of tagged arteries, but offer additional information about individual arteries. Using self-controlled ss-ASL, it is possible to reduce scan time by half compared to label-control matched images, independent of the number of arteries imaged. Compared to non-selective imaging, image acquisition time using three label images is generally longer. When acquiring additional flow territories, the scan time also increases in parallel with the number of acquired label images. This factor needs to be considered, depending on how much information about individual flow territories is needed. This could be useful in the diagnosis of individually feeding arteries in patients suffering from tumours or arteriovenous malformations [19, 20]. However, when the aim is to selectively visualise a larger number of arteries, this might lead to prolonged overall scan duration. Theoretically, the approach presented is not limited in the number of arteries to be imaged. The decoding matrix must be expanded by the number of arteries to be labelled, which is also true for other encoding/decoding patterns [21, 22].

By combining the images according to Fig. 1 (i.e. twice the label image of interest and two contralateral images) for calculating the vascular territories, rather than only two as in conventional (selective) ASL, the signal level in the contralateral arteries increases by the square root of 2, which must be accounted for [17]. As the label image of the artery of interest is added to itself, SNR remains unchanged, while the addition of the contralateral images increases SNR by the square root of 2. This means that for a quantitative analysis (i.e. using the formula in [9]), this signal change needs to be taken into account, as the absolute CBF values would otherwise be artificially too high. When only relative CBF values are of interest, this increased signal is of help in further differentiating areas of hyper- and hypoperfusion.

Setting negative values to zero in the self-controlled approach might be another source of uncertainty. Theoretically, a negative signal is not possible in voxels in which the perfusion signal is above the noise threshold. Nevertheless, this effect needs to be evaluated for pathological conditions, such as mixed perfusion.

Conventional super-selective ASL requires a separate positioning of the labelling focus of each artery of interest before the start of the measurement, which increases scan time [7]. A single planning procedure in which the labelling spot is shifted
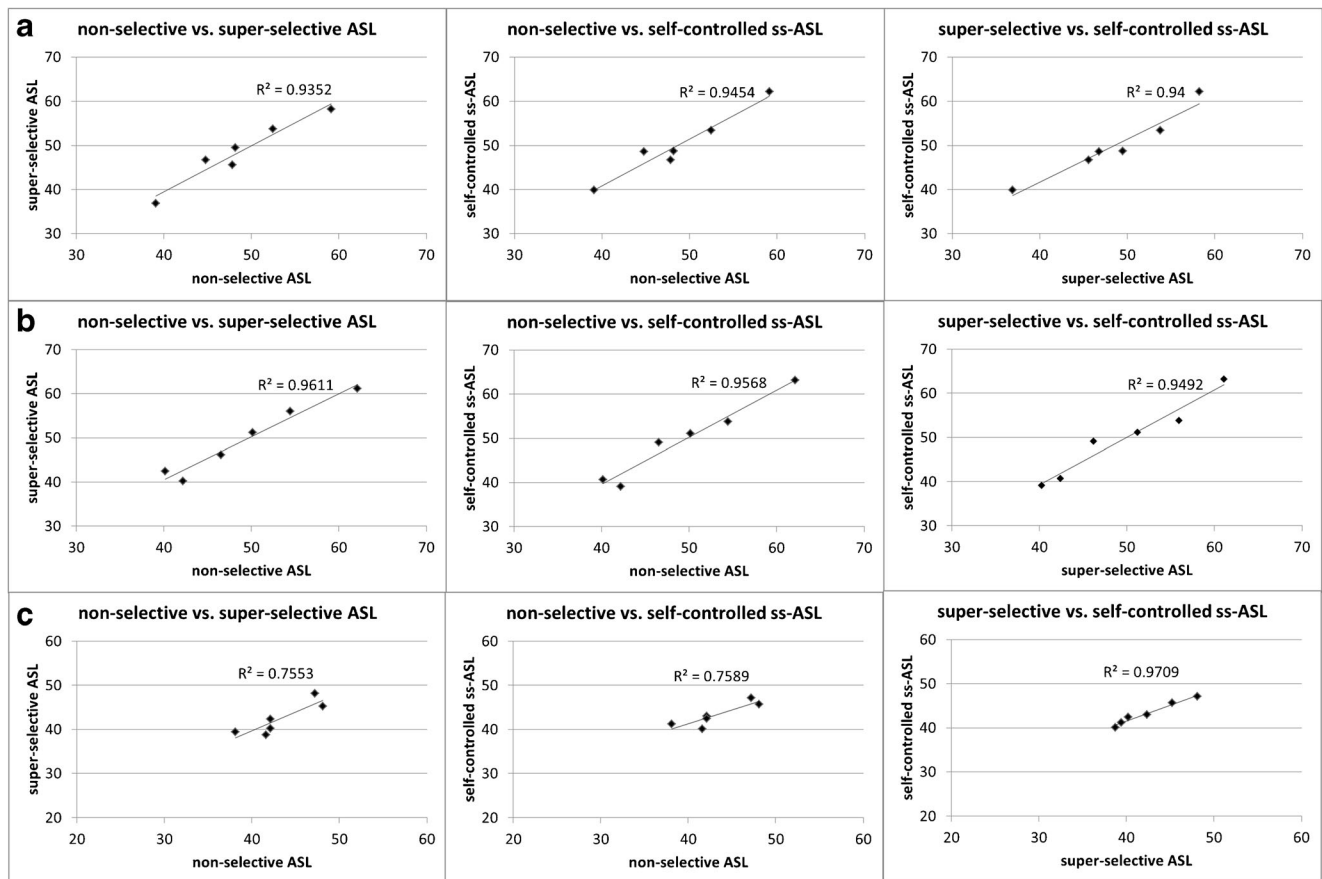
Fig. 3 Regression analysis of all presented approaches: (a) RICA, (b) LICA, (c) BA

during acquisition can make the whole planning procedure more time-efficient [11, 12]. However, movement during the scan or between planning and acquisition is still a limitation.

The applicability and reproducibility of the present method should be further evaluated in cerebrovascular diseases, which might be challenging due to altered blood flow, especially if certain flow territories are differently perfused.

To conclude, the method for self-controlled ASL presented in this work allows for non-contrast-enhanced perfusion acquisition of individual flow territories within a single scan over a shorter period of time than with conventional super-selective ASL, while the quantitative measures of perfusion do not differ significantly from those of non-selective acquisitions.

Compliance with ethical standards

Guarantor   The scientific guarantor of this publication is Prof. Dr. med. Olav Jansen.

Conflict of interest   The authors of this manuscript declare relationships with the following companies:
    Dr. Michael Helle is employed at Philips Research Laboratories, Hamburg, Germany.

Statistics and biometry   No complex statistical methods were necessary for this paper.

Informed consent   Written informed consent was obtained from all subjects (patients) in this study.

Ethical approval   Institutional review board approval was obtained.

Study subjects or cohorts overlap   Some study subjects or cohorts were previously reported in the 2016 Congress of the German Society of Neuroradiology and Congress of the 2017 International Society of Magnetic Resonance in Medicine.

Methodology
• prospective
• experimental
• performed at one institution

References

1. Jahng GH, Li KL, Ostergaard L, Calamante F (2014) Perfusion Magnetic Resonance Imaging: A Comprehensive Update on Principles and Techniques. Korean J Radiol. 15:554–577
2. Grade M, Hernandez Tamames JA, Pizzini FB, Achten E, Golay X, Smits M (2015) A neuroradiologist's guide to arterial spin labeling MRI in clinical practice. Neuroradiology. 57:1181–1202

3. Lin EC (2010) Radiation Risk From Medical Imaging. Mayo Clin Proc. 85:1142–1146

4. Jain V, Duda J, Avants B, Giannetta M, Xie SX, Roberts T, Detre JA, Hurt H, Wehrli FW, Wang DJ (2012) Longitudinal reproducibility and accuracy of pseudo-continuous arterial spin-labeled perfusion MR imaging in typically developing children. Radiology. 263:527–536

5. Lindner T, Helle M, Jansen O (2015) A Short Introduction to Arterial Spin Labeling and its Application to Flow Territory Mapping. Clin Neuroradiol. 25:211–218

6. Wong EC (2007) Vessel-encoded arterial spin-labeling using pseudocontinuous tagging. Magn Reson Med. 58:1086–1091

7. Helle M, Norris DG, Rüfer S, Alfke K, Jansen O, van Osch MJ (2010) Superselective pseudocontinuous arterial spin labeling. Magn Reson Med. 64:777–786

8. Hartkamp NS, Petersen ET, De Vis JB, Bokkers RP, Hendrikse J (2013) Mapping of cerebral perfusion territories using territorial arterial spin labeling: techniques and clinical application. NMR Biomed. 26:901–912

9. Alsop DC, Detre JA, Golay X, Günther M, Hendrikse J, Hernandez-Garcia L, Lu H, MacIntosh BJ, Parkes LM, Smits M, van Osch MJ, Wang DJ, Wong EC, Zaharchuk G (2015) Recommended implementation of arterial spin-labeled perfusion MRI for clinical applications: A consensus of the ISMRM perfusion study group and the European consortium for ASL in dementia. Magn Reson Med. 73:102–116

10. Dai W, Garcia D, de Bazelaire C, Alsop DC (2008) Continuous flow-driven inversion for arterial spin labeling using pulsed radio frequency and gradient fields. Magn Reson Med. 60(6):1488–1497

11. Günther M (2006) Efficient visualization of vascular territories in the human brain by cycled arterial spin labeling MRI. Magn Reson Med. 56:671–675

12. Lindner T, Larsen N, Jansen O, Helle M (2016) Accelerated visualization of selected intracranial arteries by cycled super-selective arterial spin labeling. Magn Reson Mater Phy. 29(6):843–852

13. von Samson-Himmelstjerna FC, Sobesky J, Chappell MA, Günther M (2015) Subtraction free arterial spin labeling : a new Bayesian-inference based approach for gaining perfusion data from time. Proc Intl Soc Magn Reson Med 2015, Toronto, CA Abstract: 0275

14. Andia ME, Botnar RM. Modified quadruple inversion recovery prepulse for arterial spin labeling angiography without the need of subtraction. J Cardiovasc Magn Reson. 2011; 13: P375.

15. Kamano H, Yoshiura T, Hiwatashi A, Yamashita K, Takayama Y, Nagao E, Sagiyama K, Zimine I, Honda H (2012) Accelerated territorial arterial spin labeling based on shared rotating control acquisition: an observer study for validation. Neuroradiology. 54:65–71

16. Helle M, Rüfer S, van Osch MJ, Jansen O, Norris DG (2012) Selective multivessel labeling approach for perfusion territory imaging in pseudo-continuous arterial spin labeling. Magn Reson Med. 68:214–219

17. Gudbjartsson H, Patz S (1995) The Rician Distribution of Noisy MRI Data. Magn Reson Med. 34:910–914

18. Chen Z, Zhang X, Yuan C, Zhao X, van Osch MJ (2016) Measuring the labeling efficiency of pseudocontinuous arterial spin labeling. Magn Reson Med. https://doi.org/10.1002/mrm.26266

19. Helle M, Rüfer S, van Osch MJ, Nabavi A, Alfke K, Norris DG, Jansen O (2013) Superselective arterial spin labeling applied for flow territory mapping in various cerebrovascular diseases. J Magn Reson Imaging. 38:496–503

20. Jensen-Kondering U, Lindner T, van Osch MJ, Rohr A, Jansen O, Helle M (2015) Superselective pseudo-continuous arterial spin labeling angiography. Eur J Radiol. 84:1758–1767

21. Teeuwisse W, Schmid S, Ghariq E, Veer IM, van Osch MJ (2014) Time-encoded pseudocontinuous arterial spin labeling: basic properties and timing strategies for human applications. Magn Reson Med. 72:1712–1722

22. Iryo Y, Hirai T, Nakamura M, Inoue Y, Watanabe M, Ando Y, Azuma M, Nishimura S, Shigematsu Y, Kitajima M, Yamashita Y (2015) Collateral circulation via the circle of Willis in patients with carotid artery steno-occlusive disease: evaluation on 3-T 4D MRA using arterial spin labelling. Clin Radiol. 70:960–965